Journal of Power Sources 226 (2013) 179–185

Contents lists available at SciVerse ScienceDirect

Journal of Power Sources

journal homepage: www.elsevier.com/locate/jpowsour

Polyelectrolyte based on tetra-sulfonated poly(arylene ether)s for direct methanol fuel cell

Jinhui Pang*, Kunzhi Shen, Dianfu Ren, Sinan Feng, Zhenhua Jiang

Alan G. MacDiarmid Institute, Department of Chemistry, Jilin University, No.2699 Qianjin Street, Changchun 130012, PR China

HIGHLIGHTS

- We synthesized novel tetra-sulfonated poly(arylene ether ketone)s as PEM materials.
- The membranes exhibited lower water uptake and swelling ratio than Nafion 117.
- Combination of considerable proton conductivity and low methanol permeability.
- The membranes are promising candidate PEM materials for direct methanol fuel cell.

GRAPHICAL ABSTRACT

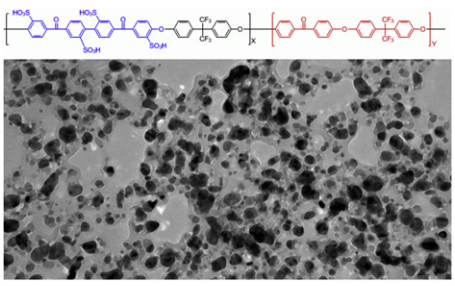

ARTICLE INFO

Article history:
Received 14 August 2012
Received in revised form
23 October 2012
Accepted 3 November 2012
Available online 10 November 2012

Keywords:
Sulfonated poly(arylene ether ketone)
Fuel cells
Direct methanol fuel cell
Proton exchange membranes

ABSTRACT

A series of tetra-sulfonated poly(arylene ether)s are prepared from a new tetra-sulfonated difluoride monomer and commercial 4,4′-difluorobenzophenone and 4,4′-(hexafluoroisopropylidene)diphenol via polycondensation process. With the content of tetra-sulfonated monomer raising from 15% to 35% in difluoride monomer, sulfonated polymers with ion exchange capacity (IEC) ranging from 0.92 to 1.66 mequiv g^{-1} are obtained. The high thermal stable polymer owns the glass transition temperature higher than 190 °C and onset decomposition temperature higher than 300 °C. The polymers exhibit good solubility in dimethylacetamide (DMAc) and the tough, flexible and transparent films are obtained by solution casting method. These membranes exhibit suitable proton conductivity, low methanol permeability and excellent dimensional stability. The membrane with $IEC_E = 1.81$ mequiv g^{-1} shows considerable proton conductivity (84 mS cm^{-1}) and swelling ration (only 8.6%) under fully hydrated state at 100 °C. Their excellent performance is attributed to distinct phase separation between hydrophilic and hydrophobic morphology, which is observed by TEM. This work demonstrates that the strategy of combining locally high densities hydrophilic segment with fluorine-containing hydrophobic segment in a polymer chain can balance on proton conduction and dimensional stability efficiently. Furthermore, these membranes own much lower methanol permeability and higher selectivity than Nafion.

1. Introduction

Polymer electrolyte fuel cells (PEFCs) are receiving increasing attention because of their high energy conversion efficiency, low emission of pollutants and low operating temperature [1]. Polymer electrolyte membranes (PEMs) have attracted considerable attention because they play the key role in PEFCs, acting as a proton transport media and as a separator of fuel and oxidant. Currently, Nafion is the most widely used proton exchange membrane [2]. However, it still shows some serious disadvantages. Hence, modified fluorine-containing membranes and aromatic membranes have been developed as alternative membranes for PEMs, due to their thermal stability, low cost, and low fuel permeability [3–8].

* Corresponding author. Tel./fax: +86 431 85168199.
E-mail address: pangjinhui@jlu.edu.cn (J. Pang).

0378-7753/$ – see front matter © 2012 Elsevier B.V. All rights reserved.
http://dx.doi.org/10.1016/j.jpowsour.2012.11.005

PEMs usually require high proton conductivity and low methanol permeability, and both factors contribute high selectivity, which shows overall performance of the membrane [9,10]. The aromatic ionomers with high ion exchange capacity (IEC) are widely used to achieve high proton conductivity, but they also have drawbacks such as high water uptake, poor dimensional stability, and increased methanol permeability [11,12]. Therefore, some strategies have been attempted to improve the selectivity under the high methanol concentration condition [13,14]. Besides, the polymers lose their mechanical stability and this limits their practical application in PEFCs. Also there is much research related to improving proton conductivity and mechanical strength by ionic cross-linked ionomer. However, it has drawbacks, such as rapidly decreased proton conductivity [15].

Many researchers have made effort to improve mechanical property and to lower methanol permeability while maintaining higher proton conductivity [16,17]. In general, the acid units of these ionomers have been concentrated to specific side chain or to polymer backbone in order to improve the nanophase separation between hydrophilic and hydrophobic domains. So far, there have been several studies on the application of much concentration sulfonated technology. Hay group reported poly(arylene ether)s ionomers with concentrated sulfonic acid segment or end cap [18–20]. Those ionomers had the same level of IECs (1.16 mequiv g^{-1}) as Nafion 117 (0.91 mequiv g^{-1}) and showed the same level of proton conductivity as Nafion 117. Guiver et al. prepared comb-shaped copoly(arylene ether)s ionomers [21–23], which exhibited organized phase-separated morphology with well-connected nanochannels, thus resulting in a dramatic enhancement in proton conductivity under partially hydrated conditions relative to other hydrocarbon-based PEMs. While Jannasch group prepared the poly(ether sulfone)s with highly sulfonated unit in the backbone or side chain [24,25]. These highly sulfonated ionomers were tailored to acquire enhanced proton conductivity, however the methanol resistance of the membranes was put aside. In addition, when sulfonated aromatic polymers serve as PEM in direct methanol fuel cell (DMFC), their methanol permeability is raised to an indispensable role.

Therefore, we aimed at designing concentrated sulfonated aromatic polymers with considerable conductivity and good methanol resistance. The present work reports the synthesis and properties of sulfonated poly(arylene ether ketone) (SPAEK) containing the nonsulfonated moiety and highly sulfonated moiety. The tetrasulfonic-containing segment can enhance sulfonic acid density in hydrophilic phase, and high fluorine-containing hydrophobic segment increases the dimensional stability of the SPAEK membranes. This approach allows a more uniform distribution of sulfonic acid group better precision with targeted IEC, and better control over the length of the statistical nonsulfonated segments, are favorable for hydrophilic/hydrophobic microphase separation morphology.

2. Experimental

2.1. Materials

Dimethyl sulfoxide (DMSO), dimethylacetamide (DMAc), toluene, sulfuric acid fuming (SO_3 >30%) and 4-fluorobenzoyl chloride were purchased from Shanghai Chemical Reagent Co., Ltd. 4,4′-(hexafluoroisopropylidene)diphenol (6FBPA), 4,4′-difluorobenzophenone (DFDPK), biphenyl and K_2CO_3 were purchased from Sinopharm Chemical Reagent Beijing Co., Ltd. Other commercially available materials and solvents were used without further purification.

2.2. Synthesis

2.2.1. Synthesis of 4,4′-bis(4-fluorobenzoyl)diphenyl (**1**)

To a 100 mL round-bottomed flask were added 4-fluorobenzoyl chloride (17.44 g, 0.11 mol), diphenyl (7.7 g, 0.05 mol), anhydrous aluminum chloride (20 g, 0.15 mol), and o-dichlorobenzene (60 mL) with stirring under nitrogen at 0 °C. The suspension was stirred at room temperature for 1 h and at 90 °C for 8 h. The reaction mixture was poured into cold aqueous hydrochloric acid, and then the water was decanted off and the residue was washed with water several times. Next, methanol was added to the oily residue to precipitate the solid. Finally, the crude product was recrystallized from DMAc and dried under vacuum at 100 °C to afford 16.9 g of white crystals (**1**). Yield: 85%; m.p. 267 °C (by DSC).

2.2.2. Synthesis of sodium 4,4′-bis(4-fluoro-3-sulfonatobenzoyl) biphenyl-2,2′-disulfonate (SDFDPK)

The synthesis of sulfonated monomer was performed according to a sodium 5,5′-carbonylbis(2-fluorobenzene-sulfonate) procedure described by Wang et al. [11]. As shown in Scheme 1, 39.8 g (0.1 mol) of 4,4′-bis(4-fluorobenzoyl)diphenyl was dissolved in 30% fuming sulfuric acid (100 mL). The solution was stirred at 110 °C for 6 h, cooled to room temperature, and poured into ice water. Excess NaOH was added to the mixture to neutralize the solution. The mixture was then incubated to room temperature and NaCl was added to precipitate the sulfonated monomer. The sulfonated monomer was finally filtered and dried in an ambient condition. The monomer was then recrystallized for three times using a mixture of ethanol and water. The yield of the sulfonation reaction is around 85%. The chemical structure of sodium 4,4′-bis(4-fluoro-3-sulfonatobenzoyl)biphenyl-2,2′-disulfonate was confirmed by Fourier transform infrared (FT-IR) and ^{1}H NMR spectroscopy. The FT-IR spectrum (KBr substrate, cm^{-1}) shows intense absorption bands at 1646 (C═O stretching), 1033 and 1089 cm^{-1} (asymmetric and symmetric stretching vibrations of sodium sulfonate groups).

The ^{1}H NMR spectrum (500 MHz, DMSO-d_6) shows peaks at J_{H1} = 8.5 ppm (d, 8.1 Hz, 2H), J_{H2} = 8.3 ppm (d, 1.4 Hz, 2H), J_{H3} = 8.1 ppm (m, 8.5 Hz, 4H), J_{H4} = 7.8 ppm (m, 2H), and J_{H5} = 7.4 ppm (t, 8.6, 9.4 Hz, 2H) where H_1–H_5 respectively represent the hydrogen atoms of the sulfonated monomer labeled in Fig. 1. These spectroscopic results confirm the formation of the sulfonated monomer.

2.2.3. Synthesis of SPAEK-x

A typical polymerization of SPAEK-*x* (*x* is the mole ratio of sulfonated moiety in a molecular chain) is shown in Scheme 2. As an example, the synthesis of SPAEK-20 is described as follows. To a round-bottomed flask equipped with a Dean-Stark trap and mechanical mixture, DFDPK (0.004 mol, 0.8728 g), 6FBPA (0.005 mol, 1.6812 g), SDFDPK (0.001 mol, 0.8066 g), and K_2CO_3 (0.0055 mol, 0.7590 g) were charged. Then DMSO (10 mL) and

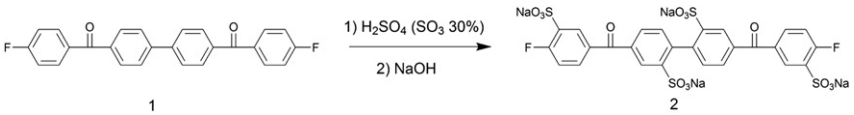

Scheme 1. Synthesis of sulfonated monomer (SDFDPK).

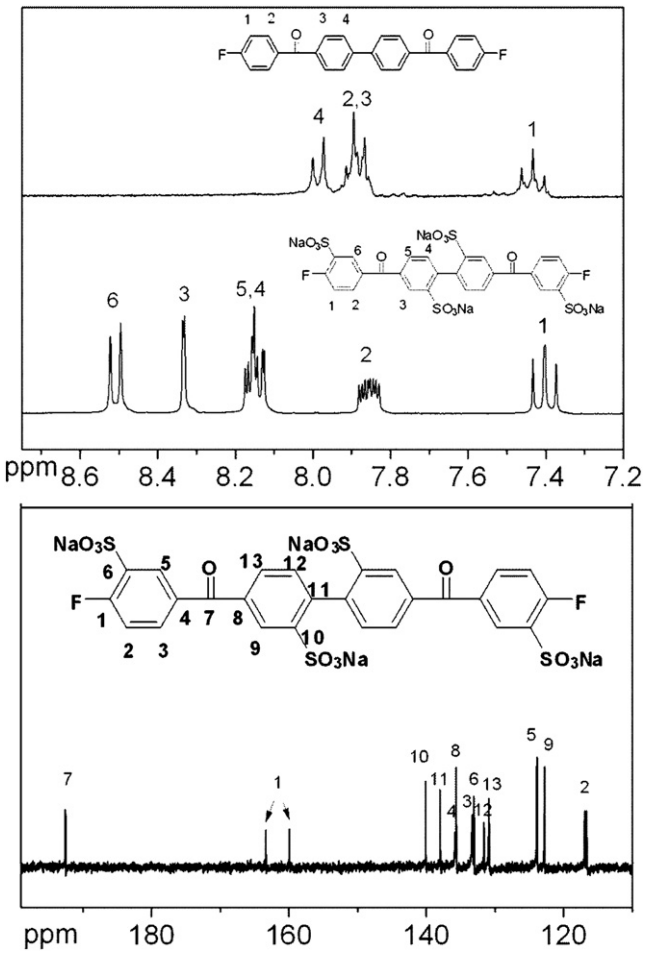

Fig. 1. ^{1}H NMR and ^{13}C NMR spectra of monomers.

toluene (5 mL) were added into the flask under argon. The reaction mixture was stirred at 140 °C for 2 h. After removal of toluene, the reaction temperature was increased to 175 °C, and continued for 6 h. After cooling to room temperature, the reaction mixture was poured in to 200 mL deionized water. The resulting flexible fiber was obtained and washed with hot deionized water and ethanol. The polymer was dried in vacuo at 120 °C for 12 h to give pure SPAEK-20 product. The yield is 97%. SPAEK-15, SPAEK-25, SPAEK-30 and SPAEK-35 were obtained in the same routine only to change the feed ratio of DFDPK and SDFDPK.

2.2.4. Membrane preparation and ion exchange capacity (IEC)

10 mL DMAc solution (10 g dL^{-1}) of a sulfonated polymer was filtered and cast on to a flat glass plate. The flat was heated at 80 °C for 12 h, 120 °C for 2 h. Then the film was dried in vacuo at 120 °C for 12 h. The dried film was immersed in 2 M H_2SO_4 solution at room temperature for over night and then thoroughly washed with deionized water for several times to give a tough and flexible membrane.

The ion exchange capacity (IEC) of the membranes was determined by titration. The membranes were immersed in saturated NaCl solution for 48 h to liberate the H^+ completely, and the free H^+ was titrated with 0.02 M NaOH solution, with phenolphthalein as indicator. The IEC values were calculated from the titration results as the ratio of the amount of NaOH consumed (mmol) to the weight of the dried membrane samples (g).

2.3. Measurements

NMR spectra were recorded on a 500 MHz Bruker510 spectrometer using deuterated dimethyl sulfoxide (DMSO-d_6) as solvent and tetramethylsilane (TMS) as internal standard. Fourier transform infrared (FT-IR) spectra (polymer thin film) were measured on a Nicolet Impact 410 Fourier transform infrared spectrometer. The intrinsic viscosities were determined from 0.5 g dL^{-1} DMAc solution of sulfonated polymer using an Ubbelohde viscometer at 25 °C. The glass transition temperature of sulfonated polymer was measured on a Mettler Toledo DSC821^e instrument at a heating rate of 10 °C min^{-1} from 50 to 280 °C under nitrogen. The thermal stability was conducted on a Perkin Elmer Pyris 1 thermal analyzer system under nitrogen from 100 to 800 °C at a heating rate of 10 °C min^{-1}.

2.3.1. Water uptake and swelling ratio measurements

Membranes were equilibrated in water for 48 h to determine the water uptake (W_{water}) and swelling ratio (S_{water}) under immersed conditions at different temperatures (20 °C, 40 °C, 60 °C, 80 °C, 100 °C). To obtain the wet weight (W_{wet}), thickness (T_{wet}) and length (L_{wet}), the excess water was gently removed with tissue paper before measuring the swollen membranes. The dry weight (W_{dry}), thickness (T_{dry}) and length (L_{dry}) were obtained after drying in vacuo at 120 °C for 24 h. The water uptake and swelling ratio were then calculated as:

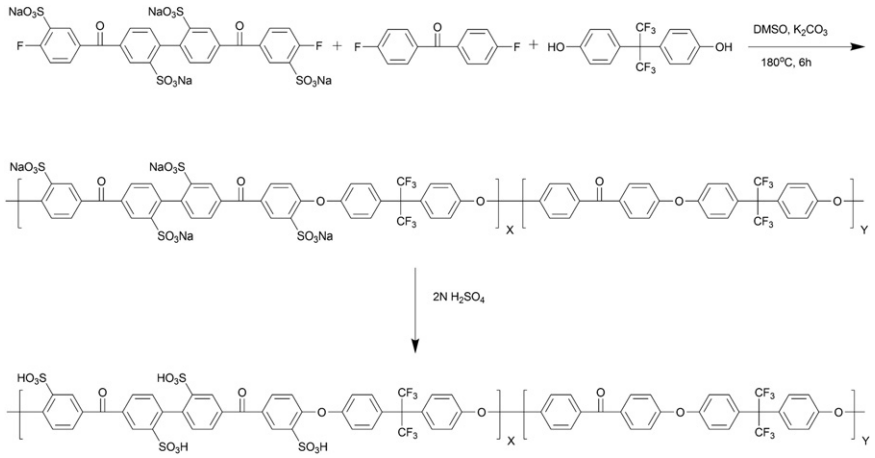

Scheme 2. Synthesis of tetra-sulfonated poly(arylene ether) copolymers (SPAEK-*x*), *x* is the mole ratio of sulfonated moiety in a molecular chain, $y=1-X$.

$$W_{water} = \left(W_{wet} - W_{dry}\right) \Big/ W_{dry} \times 100\%$$

$$S_{water}(L\%) = \left(L_{wet} - L_{dry}\right) \Big/ L_{dry} \times 100\%(\text{in-plane swelling ratio})$$

$$S_{water}(T\%) = \left(T_{wet} - T_{dry}\right) \Big/ T_{dry} \times 100\%(\text{through-plane swelling ratio})$$

2.3.2. Oxidative and hydrolytic stability

The oxidative stability of the membranes was investigated according to a typical procedure. The membrane samples (0.5 cm × 1 cm) were soaked in Fenton's reagent (3% H_2O_2 aqueous solution containing 2 ppm $FeSO_4$) for 1 h at 80 °C. The oxidative stability was evaluated by change in weight and appearance of the test sample, and the viscosities of membranes after accelerated oxidative treatment were also measured.

2.3.3. Proton conductivity and methanol permeability

Fully hydrated membranes (4 cm × 1 cm) were measured by a four-electrode AC impedance method from 0.1 Hz to 100 kHz, 10 mV AC perturbation, and 0.0 V DC rest voltage using a Princeton Applied Research Model 2273A potentiostat/galvanostat/FRA. The measurement was carried out with the cell immersed in the constant-temperature water, and the proton conductivity was determined by the equation:

$$\sigma = L/RA$$

where σ is the proton conductivity, L is the distance between the electrodes used to measure the potential (L = 1 cm), R is the membrane resistance, and A is the membrane area.

A stainless steel diffusion cell was used to measure the methanol permeability as described in the literature [26]. The cell consisted of two reservoirs that were separated by a membrane. 10 M methanol solution and deionized water were placed on each side.

Magnetic stirrers were used in each compartment to ensure uniformity. The concentration of the methanol in the water reservoir was determined by using a SHIMADZU GC-8A chromatograph. The methanol permeability was calculated using the following equation:

$$C_B(t) = ADKC_A(t - t_0)/V_B L$$

where A (in cm^2), L (in cm), and V_B (in mL) are the effective area, the thickness of the membranes, and the volume of the permeated reservoirs, respectively. C_A and C_B (in mol m^{-3}) are the methanol concentration in the feed and in the permeate, respectively. DK (in $cm^2\ s^{-1}$) denotes the methanol permeability.

2.3.4. Mechanical properties

The mechanical properties of wet membranes were measured at room temperature on SHIMADIU AG-I 1KN at a strain rate of 2 mm min^{-1}. The size of samples was 20 mm × 4 mm. The samples in wet state were obtained by immersing them in water for 12 h.

2.3.5. Morphology

For transmission electron microscopy (TEM) observations, the membranes were stained with lead ions by ion exchange of the sulfonic acid groups in 0.5 M lead acetate aqueous solution, rinsed with deionized water, and dried in vacuum oven for 12 h. The stained membranes were embedded in epoxy resin, sectioned to 90 nm thickness with Leica microtome Ultracut UCT, and placed on copper grids. Electron micrographs were taken with a made on a JEM-1200EX electron microscope.

3. Results and discussions

3.1. Synthesis of monomer (SDFDPK)

A new difluoride monomer with four sulfonic acid groups was successfully obtained via two synthetic procedures. The first, 4,4′-bis(4-fluorobenzoyl)diphenyl (**1**) was synthesized from 4-fluorobenzoyl chloride and diphenyl by Friedel–Carfts reaction. Then sulfonation of **1** was performed using fuming sulfuric acid to give objective SDFDPK. The structure of SDFDPK was confirmed by NMR spectroscopy. The ^{1}H NMR spectrum of SDFDPK is shown in Fig. 1. Compared with monomer **1**, the proton signal peaks of SDFPK become complex, due to strong electron withdraw sulfonic acid groups are present. ^{13}C NMR was also used to confirm structure of SDFPK furthermore (Fig. 1), and the carbon signal peaks were assigned well.

3.2. Synthesis of sulfonated polymer

The tetra-sulfonated poly(arylene ether ketone)s named SPAEK-*x* were synthesized via K_2CO_3-catalyzed classical aromatic nucleophilic substitution polycondensation of SDFDPK, DFDPK, and 6FBPA in DMSO solution. The obtained sulfonated polymers were readily soluble in polar aprotic solvents such as NMP, DMAc, and DMF. And inherent viscosity of SPAEK-*x* in DMAc at 25 °C ranged from 1.7 to 2.0 dL g^{-1} indicating their high molecular weights. The tough, flexible, and transparent membranes of SPAEK-*x* were obtained by solvent casting. The thickness of these membranes is shown in Table 1.

FT-IR and ^{1}H NMR were used to confirm structure of SPAEK-*x*. In FT-IR spectra of SPAEK-*x*, the absorption bands at 1084 and 1030 cm^{-1} are corresponding to asymmetric and symmetric vibration of sulfonic acid groups, respectively. And the absorption band at 1656 cm^{-1} is assigned to diphenylcarbonyl vibration. As shown in Fig. 2, the ^{1}H NMR spectra of SPAEK-15 and SPAEK-35 were assigned clearly. The protons H_3, H_1, H_5, and H_2 in sulfonated segment appear at high chemical shift (8.0–8.6 ppm), due to the effect of electron-withdrawing groups. The FT-IR and ^{1}H NMR signals of the SPAEK are corresponding to polymer structure feature, which demonstrates that the objective sulfonated copolymers were obtained successfully.

Table 1
Basic properties of sulfonated polymer SPAEK-*x*.

Polymer	*X*	DS [a]	IEC_C [b] (mequiv g^{-1})	IEC_E [c] (mequiv g^{-1})	T_g (°C)	$T_{d\ onset}$ (°C)	$T_{d\ 5\%}$ (°C)	[ŋ] [d] (dL g^{-1})	Thickness [e] (μm)	Tensile strength (MPa)	Elongation at break (%)
SPAEK-35	0.35	1.4	2.00	1.81	231	333	364	1.7	103	44	38
SPAEK-30	0.30	1.2	1.80	1.63	219	335	369	1.8	95	54	74
SPAEK-25	0.25	1.0	1.50	1.36	205	339	371	2.0	88	58	90
SPAEK-20	0.20	0.8	1.40	1.28	200	341	378	1.9	87	61	110
SPAEK-15	0.15	0.6	1.00	0.93	193	332	390	1.8	81	53	110

[a] DS (degree of sulfonation) refers to the number of sulfonic acid group on every polymer repeat unit.
[b] IEC_C: Theoretical value.
[c] IEC_E: The data from titration method.
[d] Measured at a concentration of 0.5 g dL^{-1} in DMAc at 25 ± 0.1 °C.
[e] Membranes prepared by DMAc solution casting method.

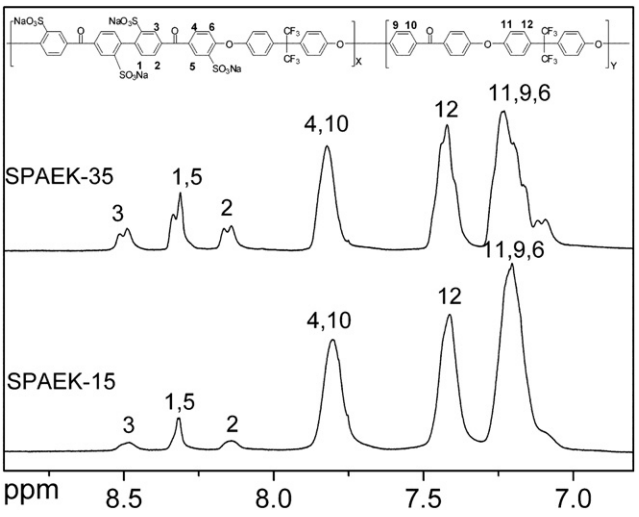

Fig. 2. ^{1}H NMR spectra of the sulfonated poly(arylene ether ketone)s (SPAEK-*x*).

3.3. Thermal stability of SPAEK-x

SPAEK-*x* copolymer exhibited excellent thermal stability. The onset weight loss temperature is above 330 °C, and 5% weight loss higher than 360 °C (Table 1). The TGA curves of SPAEK-*x* are shown in Fig. 3, a two-step degradation profile was observed. The first weight loss at about 300 °C was attributed to the elimination of sulfonic acid groups, while the second weight loss at about 500 °C was due to the degradation of the main chain of sulfonated copolymers. The high decomposition temperature suggests that sulfonic groups attached to carbonyl-passivated benzene ring have high thermal stability. The DSC curves of SPAEK-*x* are displayed in Fig. 3, and the glass transition temperatures (T_gs) increase with an elevated IEC values. As seen in Table 1, all the T_gs of the SPAEK were around 200 °C, which are much lower than the decomposition temperature. This facilitates the preparation of the MEA by hot pressing.

3.4. IEC, water uptake and swelling ratio

Ion exchange capacity (IEC) value is very closely related to dimensional stability and proton conductivity of PEM under fuel cell operation condition. Although, the level of hydration of proton exchange membranes is highly dependent on the IEC, at high levels of hydration the mechanical properties are typically compromised and acid concentration is reduced because of the high water uptake and swelling ratio. Thus SPAEK-*x* was designed to prepare with appropriate IEC values between 1.0 and 2.0 mequiv g^{-1}. And the experimental IEC_E values of SPAEK-*x* were determined by titration and agreed well with calculated values (Table 1).

In general, the membranes of sulfonated poly(arylene ether)s exhibited a high water uptake over than 80% and large swelling ratio over than 25% when IEC around 2.0 mequiv g^{-1}. Although, SPAEK-35 with high IEC_E (1.81 mequiv g^{-1}) exhibited relatively low water uptake (23.5%) and excellent resistance to hot water since the swelling ratio (in-plane direction) is only 5.1% at 80 °C. Those advantages are attributed to their special structure that the functional sulfonic acid group concentrated distribution in a part of backbone leader to fluorine-containing hydrophobic segments became longer. As a result, SPAEK-*x* membranes possess an effective proton transport channel and have a very stable hydrophobic phase even in hot water. Fig. 4 shows the water uptake and swelling ratio (in-plane direction) of SPAEK-*x* membranes as a function of

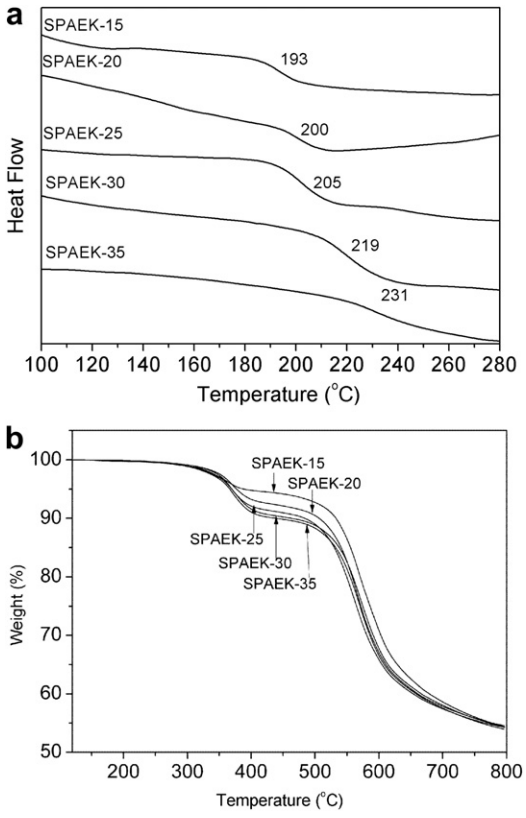

Fig. 3. (a) DSC curves of the SPAEK-*x*; (b) TGA curves of the SPAEK-*x*.

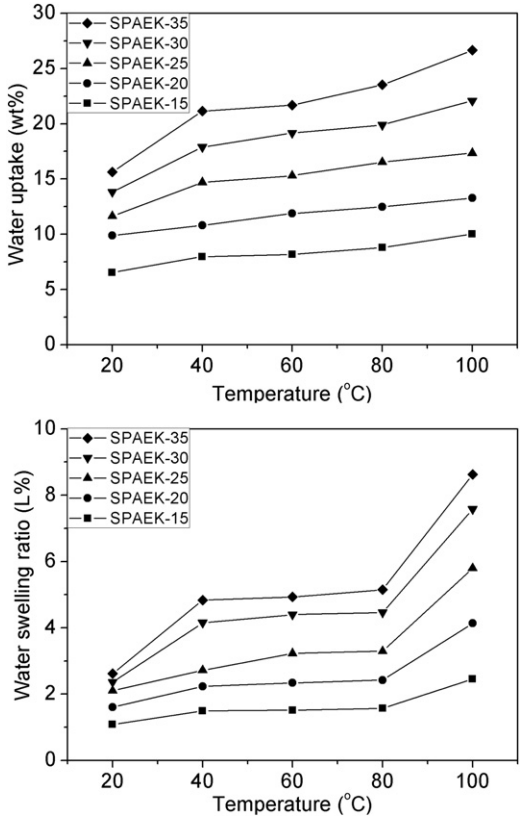

Fig. 4. Water uptake and water swelling ratio (in-plane direction) of SPAEK-*x* film as a function of temperature.

temperature. The water uptake and swelling ratio both increase with IEC and temperature increased. In general, highly sulfonated aromatic membranes can format a larger and more continuous ion network when temperature over 80 °C, thus the water sorption and swelling ratio increase sharply [11]. More interestingly, the water uptake and swelling of SPAEK-*x* exhibited both mild increases even at high temperature. In addition, in boiling water the water uptake and swelling ratio (in-plane direction) of those membranes were less than 27% and 9%, respectively.

3.5. Oxidative stability and mechanical properties

The oxidative stability of the membranes SPAEK-*x* was evaluated in a hot Fenton's reagent (80 °C) for 1 h as an accelerated test. The results are summarized in Table 2. For all samples, almost no weight loss was observed, and their film properties such as flexibility and transparency were maintained even after the test. While the viscosities of treated membranes slightly decreased, and SPAEK-35 membrane displayed a reduced viscosity of 1.3 dL g^{-1} after oxidative stability test. As a result, although those polymers exhibited no changes in appearance after this test, the degradation behavior has occurred on the polymer segment, especially at high IEC level.

It is essential for PEM to possess adequate mechanical strength under dry and humidified conditions. Here, the tensile test of membranes was conducted at ambient conditions with relative humidity (RH) about 80%, and the results are summarized in Table 1. The strength for the membranes of SPAEK-15, SPAEK-20, SPAEK-25, SPAEK-30, and SPAEK-35 are 53 MPa, 61 MPa, 58 MPa, 54 MPa, and 44 MPa, respectively, which are higher than that of Nafion 117. All five SPAEK(-15, -20, -25, -30, -35,) showed elongation at break of 110%, 110%, 90%, 74%, and 38%, respectively. These data indicate these membranes are strong, tough and flexible at RH 80% and are very promising.

3.6. Proton conductivity and methanol permeability

As a polymer electrolyte, the proton conductivity is an important index. A lot of aromatic proton exchange membranes have been reported because of their suitable proton conductivity. However poor dimensional stability of the membranes has restricted their application. In general, the proton conductivity of membranes rich to $\sim 10^{-2}$ S cm^{-1} can be used as a polyelectrolyte material [3]. The proton conductivity of SPAEK-*x* was measured under immersed conditions. Those membranes have moderate proton conductivity, which are higher than 10^{-2} S cm^{-1} over the full test temperature range. As seen in Table 2, SPAEK-35 shows twenty times proton conductivity higher than SPAEK-6F-20 membrane at the similar swelling level. On the other hand, at the similar proton conduction level ($\sim$30 mS cm^{-1}, 80 °C), the SPAEK-25 exhibited a swelling ratio of 3.3% very less than SPAEK-6F-40 of 9%. The results illuminate that the proton conductivity and swelling of SPAEK-*x* membranes were affective balanced by controlling hydrophilic/hydrophobic morphology. As shown in Fig. 5, the proton conductivity of SPAEK-*x* membranes was measured as a function of temperature. The proton conductivities increased with IEC and temperature increasing. Due to high IEC value, the SPAEK-35 membrane showed the highest conductivity than that of other membranes over the entire temperature range studied. And the proton conductivities of SPAEK-35 membrane are 35 and 84 mS cm^{-1} at 40 and 100 °C, respectively. The results indicate that they are potential candidate for PEM material.

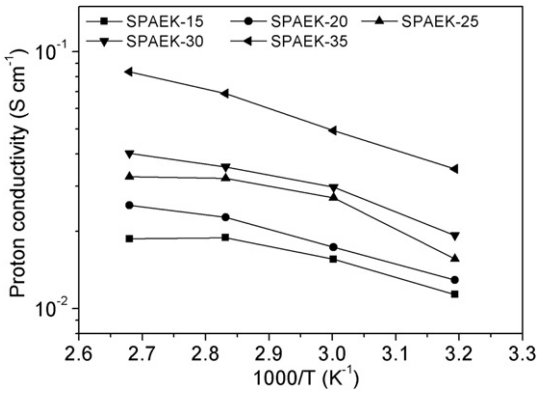

Fig. 5. Proton conductivity of SPAEK-*x* films as a function of temperature.

Membranes used in DMFCs must possess high proton conductivity and be an effective barrier for methanol crossover from the anode to the cathode compartment. The methanol permeability of SPAEK-*x* is summarized in Table 2. As the IEC and liquid uptake increased, the methanol permeability of SPAEK-*x* membranes increased from 4.38×10^{-9} cm^2 s^{-1} to 5.08×10^{-8} cm^2 s^{-1} at room temperature, which is significantly lower than that of the Nafion 117 membrane (1.65×10^{-6} cm^2 s^{-1}). Fig. 6 shows the relationship of proton conductivity and the inverse of methanol permeability of SPAEK-*x* membranes. All of the membranes, with low methanol permeability, located on the right-hand side of the line. This indicates that the membranes possess suitable proton conductivity and low methanol permeability. In addition, a metric for selecting a high performance fuel cell membrane is its electrochemical selectivity [27]. The selectivity of a membrane is defined as the ratio of proton conductivity and methanol permeability. The relative selectivity is then the selectivity of the membrane divided by the selectivity of Nafion 117. Compared to some earlier literature [28–30], these SPAEK membranes exhibited 3–4 times higher selectivity (shown in Table 2). The excellent methanol resistance and selectivity made them promising materials for DMFC applications.

Table 2
The water absorption, conductivity, oxidative stability, methanol permeability and selectivity of SPAEK-*x*.

Polymer	W_{water} (wt%)		S_{water} (L%)		S_{water} (T%)		σ (mS cm^{-1})	Oxidative stability (%)	Methanol permeability (cm^2 s^{-1})	Relative selectivity [b]
	RT	80 °C	RT	80 °C	RT	80 °C	80 °C			
SPAEK-35	15.6	23.5	2.6	5.1	7.6	10.9	68.8	99.8	5.08×10^{-8}	13.7
SPAEK-30	13.8	19.8	2.4	4.5	5.8	6.8	35.7	99.9	2.94×10^{-8}	13.1
SPAEK-25	11.6	16.5	2.1	3.3	4.8	6.3	32.1	100	2.31×10^{-8}	13.4
SPAEK-20	9.9	12.4	1.6	2.4	3.2	4.8	22.7	100	1.97×10^{-8}	12.9
SPAEK-15	6.5	8.7	1.1	1.6	2.9	3.8	18.9	100	4.38×10^{-9}	51.5
[a]SPAEK-6F-40	17	25	6	9	–	–	30	–	–	–
[a]SPAEK-6F-20	8	10	3	5	–	–	2.8	–	–	–

[a] Data from reference [17].
[b] Relative selectivity = membrane selectivity/Nafion selectivity (Selectivity = [proton conductivity]/[methanol permeability]) at 20 °C.

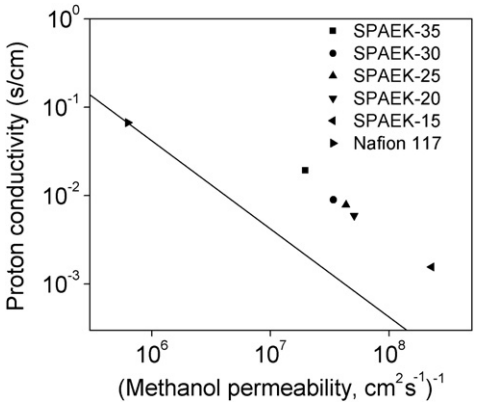

Fig. 6. Proton conductivity versus methanol permeability of SPAEK-*x* films at room temperature.

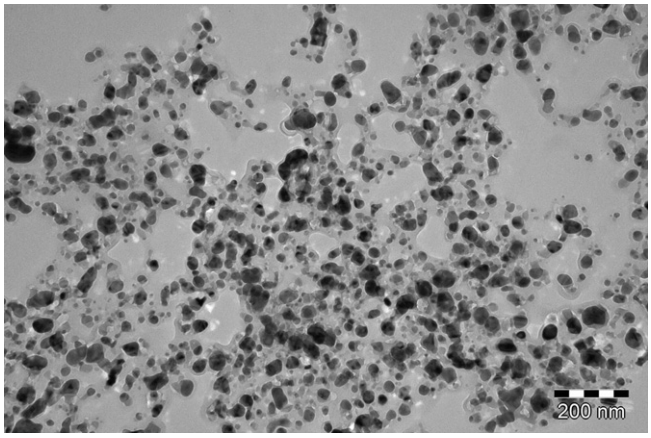

Fig. 7. The TEM image of SPAEK-35.

3.7. Morphology

The hydrophilic–hydrophobic microphase separation morphology is particularly important for PEM materials because it affects the water uptake and the proton transport pathway in the PEM. The morphology of sulfonated polymer SPAEK-35 was investigated by transmission electron microscopy (TEM) for the membranes stained with silver ions. As is clearly seen in Fig. 7, SPAEK-35 exhibited spherical ionic clusters (dark areas), diameter is around 20 nm, which is much higher than that of Nafion 117 (~8 nm) [8]. This kind of hydrophilic/hydrophobic microphase separation morphology may explain their suitable proton conductivity, low water uptake and excellent dimensional stability compared to those of the random copolymers.

4. Conclusions

A novel tetra-sulfonated unit-containing poly(arylene ether ketone) copolymer was successfully prepared by direct copolymerization from a new four sulfonic-containing difluoride monomer (SDFDPK), 6FBPA, and DFDPK. The tetrasulfonic-containing SDFDPK can enhance sulfonic acid density in hydrophilic phase, and high fluorine-containing hydrophobic segment increases the dimensional stability of the SPAEK-*x* membranes. The structures of obtained monomer and copolymers were confirmed by ^{1}H NMR spectroscopy. The tough, flexible and transparent sulfonated membranes (SPAEK-*x*) were obtained by solution casting method, and showed good thermal stability and mechanical properties. Membranes based on these ionomers exhibited suitable proton conduction at moderate water uptake and swelling ratio lower than 9%. In addition, these membranes exhibited low methanol permeability at high concentration methanol solution at room temperature. TEM image confirmed that stable hydrophilic/hydrophobic microphase separation morphology exists in SPAEK-35 membrane. The combination of good thermal stability, high proton conductivity, low methanol permeability, and excellent dimensional stability makes SPAEK-*x* attractive as PEM for DMFC applications.

Acknowledgements

The authors would like to thank the China Natural Science Foundation (Grant No: 51103060); Jilin University Basic Research Founding (No: 450060441057) for financial support of this work.

References

[1] W. Vielstich, A. Lamm, H.A. Gasteiger, Handbook of Fuel Cell: Fundamentals, Technology, and Applications, Wiley, 2003.
[2] Z. Chai, C. Wang, H. Zhang, C.M. Doherty, B.P. Ladewig, A.J. Hill, H. Wang, Adv. Funct. Mater. 20 (2010) 4394–4399.
[3] M.A. Hickner, H. Ghassemi, Y.S. Kim, B.R. Einsla, J.E. McGrath, Chem. Rev. 104 (2004) 4587–4612.
[4] H. Zhang, P.K. Shen, Chem. Rev. 112 (2012) 2780–2832.
[5] R. Souzy, B. Ameduri, Prog. Polym. Sci. 30 (2005) 644–687.
[6] C.H. Lee, S.Y. Lee, Y.M. Lee, S.Y. Lee, J.W. Rhim, O. Lane, J.E. McGrath, ACS Appl. Mater. Interfaces 1 (2009) 1113–1121.
[7] M. Rikukawa, K. Sanui, Prog. Polym. Sci. 25 (2000) 1463–1502.
[8] C.H. Parka, C.H. Lee, M.D. Guiver, Y.M. Lee, Prog. Polym. Sci. 36 (2011) 1443–1498.
[9] J. Pang, H. Zhang, X. Li, Z. Jiang, Macromolecules 40 (2007) 9435–9442.
[10] Y. Zhu, S. Zieren, A. Manthiram, Chem. Commun. 47 (2011) 7410–7412.
[11] F. Wang, T.L. Chen, J.P. Xu, Macromol. Chem. Phys. 199 (1998) 1421–1426.
[12] Q. Tang, Y. Li, Z. Tang, J. Wu, J. Lin, M. Huang, J. Mater. Chem. 21 (2011) 16010–16017.
[13] T.A. Kim, W.H. Jo, Chem. Mater. 22 (2010) 3646–3652.
[14] D. Chen, S. Wang, M. Xiao, Y. Meng, A.S. Hay, J. Mater. Chem. 21 (2011) 12068–12077.
[15] L. Fu, G. Xiao, D. Yan, J. Mater. Chem. 22 (2012) 13714–13722.
[16] T. Higashihara, K. Matsumoto, M. Ueda, Polymer 50 (2009) 5341–5357.
[17] P. Xing, G.P. Robertson, M.D. Guiver, S.D. Mikhailenko, S. Kaliaguine, Macromolecules 37 (2004) 7960–7967.
[18] S. Tian, Y. Meng, A.S. Hay, J. Polym. Sci. Part A: Polym. Chem. 47 (2009) 4762–4773.
[19] S. Matsumura, A.R. Hlil, C. Lepiller, J. Gaudet, D. Guay, A.S. Hay, Macromolecules 41 (2008) 277–280.
[20] S. Matsumura, A.R. Hlil, C. Lepiller, J. Gaudet, D. Guay, Z. Shi, S. Holdcroft, A.S. Hay, Macromolecules 41 (2008) 281–284.
[21] T.B. Norsten, M.D. Guiver, J. Murphy, T. Astill, T. Navessin, S. Holdcroft, B.L. Frankamp, V.M. Rotello, J. Ding, Adv. Funct. Mater. 16 (2006) 1814–1822.
[22] N. Li, D.S. Hwang, S.Y. Lee, Y.L. Liu, Y.M. Lee, M.D. Guiver, Macromolecules 44 (2011) 4901–4910.
[23] N. Li, C. Wang, S.Y. Lee, C.H. Park, Y.M. Lee, M.D. Guiver, Angew. Chem. Int. Ed. 123 (2011) 9324–9327.
[24] B. Lafitte, P. Jannasch, Adv. Funct. Mater. 17 (2007) 2823–2834.
[25] E.P. Jutemar, S. Takamuku, P. Jannasch, Polym. Chem. 2 (2011) 181–191.
[26] B. Jung, B. Kim, J.M. Yang, J. Membr. Sci. 245 (2004) 61–69.
[27] B.S. Pivovar, Y. Wang, E.L. Cussler, J. Membr. Sci. 154 (1999) 155–162.
[28] B. Liu, G.P. Robertson, D.-S. Kim, M.D. Guiver, W. Hu, Z. Jiang, Macromolecules 40 (2007) 1934–1944.
[29] Y.-H. Su, Y.-L. Liu, D.-M. Wang, J.-Y. Lai, M.D. Guiver, B. Liu, J. Power Sources 194 (2009) 206–213.
[30] D.-S. Kim, Gilles P. Robertson, Y.S. Kim, M.D. Guiver, Macromolecules 42 (2009) 957–963.